remote sensing

MDPI

Article

Hydrological Connectivity Improves the Water-Related Environment in a Typical Arid Inland River Basin in Xinjiang, China

Chuanxiu Liu [1,2], Yaning Chen [1,*], Gonghuan Fang [1], Honghua Zhou [1], Wenjing Huang [1,2], Yongchang Liu [1,2], Xuanxuan Wang [1,2] and Zhi Li [1]

[1] State Key Laboratory of Desert and Oasis Ecology, Xinjiang Institute of Ecology and Geography, Chinese Academy of Sciences, Urumqi 830011, China
[2] Department of Resources and Environment, University of China Academy of Sciences, Beijing 100049, China
* Correspondence: chenyn@ms.xjb.ac.cn

Abstract: Hydrological connectivity directly affects aquatic ecological processes, water environment and wetland ecological security, which is essential to the stability of arid ecosystems. However, the mechanism between hydrological connectivity and water-related environment has not been revealed completely. To address these issues, we use a landscape connectivity approach to assess the connectivity of water patches for analyzing the hydrological connectivity of the Bosten Lake Basin (BLB), as well as its response to human activities and climate change, based on the Joint Research Centre (JRC) global surface water dataset. It shows that the integral index of connectivity (IIC) of the BLB is low (ranging from 0 to 0.2) from 1990 to 2019, with an increasing interannual trend. The connectivity is higher in wet periods and in oases compared with dry periods and high-altitude mountain regions. Correlation and regression analyses indicate that hydrological connectivity has a strong correlation ($r > 0.5$, $p \leq 0.05$) with water area and water level. The interannual and seasonal trends of eight hydrochemical indices in the Bosten Lake have been investigated to systematically elaborate the complex relationships between hydrological connectivity and water quality in the BLB. Results indicated that better hydrological connectivity can improve water quality, and the minimum of pollutants were observed in high hydrological connectivity period, covering approximately 75% of the high-water quality period. These findings could provide scientific support for the water management in the BLB.

Keywords: hydrological connectivity; water quality; arid region; Bosten Lake; inland river-lake systems

Citation: Liu, C.; Chen, Y.; Fang, G.; Zhou, H.; Huang, W.; Liu, Y.; Wang, X.; Li, Z. Hydrological Connectivity Improves the Water-Related Environment in a Typical Arid Inland River Basin in Xinjiang, China. *Remote Sens.* **2022**, *14*, 4977. https://doi.org/10.3390/rs14194977

Academic Editors: Songhao Shang, Qianqian Zhang, Dongqin Yin and Hamza Gabriel

Received: 6 September 2022
Accepted: 30 September 2022
Published: 6 October 2022

1. Introduction

Rivers fluctuate back and forth between dry and wet periods in arid regions [1]. The emergence and disappearance of water patches provide necessary connectivity for river and lake ecosystems, which also provide connecting pathways for biological habitats in both space and time. However, climate change and human activities bring great uncertainty to the hydrological processes and ecological changes in arid zones [2–5], which may increase the extreme precipitation and the degree and frequency of droughts [6]. Thus, they will change the flow state and river morphology of inland rivers [7,8], and weaken or even isolate the hydrological connectivity processes between rivers and lakes [9,10]. That will lead to deterioration of hydrological environment and water quality as well as a rapid decline in essential ecosystem services [11], such as lake shrinkage, water pollution, and loss of biodiversity [12–14].

Hydrological connectivity is widely defined as the water-mediated transfer of material, energy, and/or organisms within or between elements of the water cycle [15–18]. Recently, with the concept of hydrological connectivity having attracted much attention among geoscientists [19,20], theories and methods related to landscape connectivity have

been introduced into hydrology and widely used in current hydrological connectivity studies [21–23]. Hydrological connectivity describes the connectivity of lake ecosystems to terrestrial ecosystems through sedimentation, soil leaching, diffusion in wetlands, lake and river inputs (receiving water) and outputs (discharging water) [24–26]. The ability of water to exchange pollutants between different water patches depends on their connectivity with each other, and the rate of water exchange depends on the degree of connectivity between patches [25,27–30]. Hydrological connectivity determines the ability of species spread and gene flow [31,32], which is an important driver for maintaining healthy ecosystem function and social development in arid areas [33–35], and it is also important to protect biodiversity and maintain the stability as well as the integrity of natural ecosystems [36].

The fragmentation of water systems in arid inland river basins has caused the decline in hydrological connectivity, which has directly resulted in deterioration of water environment and ecological conditions. Previous studies have investigated the effects of topography, geomorphology, and human activities on hydrologic connectivity by means of graph theory, hydrologic models, and connectivity indices [21,25,37–39]. However, the relationships between fragile and irreversible ecosystems and hydrological connectivity in arid zones are still unclear due to discontinuous monitoring data and incomplete monitoring networks [6]. Meanwhile, only a few studies have focused on the correlation between water quality and hydrological connectivity [25,29,40], and they all concentrate on the relationship between hydrological connectivity and a single environmental factor [37,41–43]. Few studies attempt to explore the complex relationship between hydrological connectivity and multiple environmental factors [27,44,45]. Therefore, it is particularly urgent to investigate the response between water quality and hydrological connectivity in arid areas.

The Bosten Lake, together with the Kaidu River and the Konqi River, constitutes the Bosten Lake Basin (BLB), which is a typical inland river basin in the arid zone and one of the headwaters of the Tarim River Basin, the largest inland river basin in China [46,47]. With climate change and increased human activity, the Bosten Lake has gradually become a mesotrophic lake due to extensive salinization caused by large-scale agricultural irrigation and water diversion projects for industrial development [28,48,49]. To enhance the capacity of the water environment, a series of water system connectivity projects was implemented in recent years to improve the water quality of the Bosten Lake. As most of the surrounding tributaries of the lake are seasonal rivers, and the change in hydrological connectivity may have a significant impact on the Bosten Lake, which connects with the upstream and downstream of the basin, but these effects have never been assessed. Therefore, this study aims to (1) assess the interannual and seasonal variability characteristics of the connectivity among water patches in the BLB from 1990 to 2019; (2) analyze the characteristics of hydrochemistry changes; (3) clarify the relationship between hydrological connectivity and its water-related environmental effects. It is intended to provide a comprehensive framework to explain the hydrological connectivity and ecological response. The results of the study can provide a reference for the implementation of hydraulic engineering in inland river basins of arid regions, which is important for maintaining the stability of oasis-desert ecosystems and the integrity of river functions, and promoting the sustainable development of the region.

2. Material and Methods

2.1. Study Area

The BLB mainly includes the Kaidu River, the Konqi River, and the Bosten Lake, which is the largest inland freshwater lake in China [50]. The basin is located in the arid and semi-arid region in China. It spans an area of approximately 90,944.24 km^2 [51]. The total annual precipitation is only 76.1 mm; however, evaporation amounts to 2000 mm $year^{-1}$ [50]. A total of 65% of rainfall and 70% of evaporation happen between May and August [52]. As shown in Figure 1, the watershed has a complex topography, with mountains, oases, and desert interspersed, which is representative of a typical mountain-oasis-desert complex ecosystem. Based on the extent and characteristics of the study area, we divided it into three

sub-basins: the upper and middle reaches of the Kaidu River (KDH), the lower reaches of the Kaidu River and upper reaches of the Konqi River (KKH), and the middle and lower reaches of the Konqi River (KQH). In terms of primary topographical features, KDH is a high-altitude mountainous area, KKH is a densely populated area, and KQH includes part of the desert area.

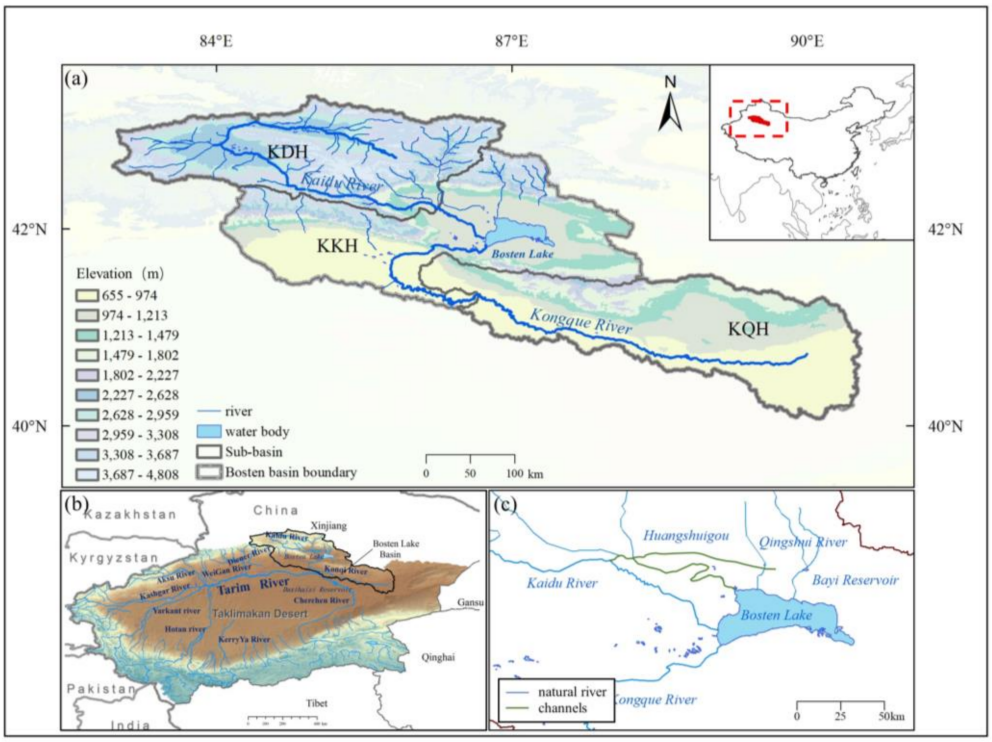

Figure 1. Location and overview of the Bosten Lake Basin. Scale and overview of the whole Bosten Lake Basin (**a**), location of the catchment within Tarim River Basin (**b**), enlarged view of the Bosten Lake (**c**).

2.2. Data

2.2.1. Remote Sensing Data

JRC Yearly Water Classification History, v1.3 (JRC-Yearly), and JRC Monthly Water Classification History, v1.3 (JRC-Monthly) are used to extract the yearly and monthly surface water body information. Both datasets contain information on the location and temporal distribution of surface water from 1984 to 2020, which provides statistical data about the extent and variability of these water surfaces [53]. These data were generated based on Landsat 5–8 imagery data, using expert systems, visual analytics, and evidential reasoning to classify each pixel individually as water body or non-water body. The results were then collated into monthly-scale for two time periods to detect water body changes, which are widely used in studies related to terrestrial hydrology [54,55].

The JRC Yearly Water Classification History, v1.3 (JRC-Yearly) collection preserves yearly water body distributions from 1984 to 2019 and contains 36 images in total, which has a spatial resolution of 30 m. Among them, there are many missing patches in the study area before 1990, so we selected all the 30 images based on the JRC-Yearly from 1990 to 2019 to identify the water area in the BLB. The JRC-Yearly dataset classifies land as permanent water, seasonal water, and others throughout the year.

The JRC Monthly Water Classification History, v1.3 (JRC-Monthly) collection preserves monthly water body distributions from 1984 to 2020 and contains 442 images in total, which have a spatial resolution of 30 m. Among them, monthly-scale water bodies have a large number of missing cases prior to 2000, and open water bodies in November-March show as ice in BLB [51], resulting in a large bias in water area statistics. To avoid large biases

skewing our results, we extracted the distribution of the water area for the months of April to October from 2000 to 2019 based on the JRC-Monthly. The JRC-Monthly The JRC-Monthly dataset classifies land as water, not water and others for the month.

2.2.2. Ecological and Hydrochemical Data

The water level and water quality data for the Bosten Lake were provided by the Bosten Lake Administration of Bayingol Mongolian Autonomous Prefecture (Xinjiang). The hydrological data includes the Bosten Lake level (BLL) data from 1990 to 2019. To investigate the relationship between hydrological connectivity and the water environmental quality of the Bosten Lake comprehensively, eight pollutions indices from 2001 to 2019 are collected from the local ecological and environmental bureau. The eight indices are: dissolved oxygen (DO), permanganate index (COD_{MN}), chemical oxygen demand (COD), five-day biochemical oxygen demand (BOD_5), total phosphorus (TP), total nitrogen (TN), ammonia nitrogen (NH3-N), and total dissolved salts (TDS) or mineralization.

2.2.3. Hydro-Meteorological Data

The hydro-meteorological data used in this study are from the Terra Climate (TC) dataset (http://www.climatologylab.org/, accessed on 1 September 2021). Three variables are selected: temperature (TMP), actual evapotranspiration (ETa), and precipitation (PREC). The TC dataset, which compiles global land surface monthly-scale climate data covering 1958–2019, is a high-precision climate dataset with 4 km (1/24 degree) spatial resolution. It combines the high spatial resolution WorldClim dataset with the low spatial resolution CRU Ts4.0 and the Japanese 55-year Reanalysis (JRA55) meteorological data [56].

2.2.4. Socioeconomic Data

The population data come from the WorldPop Global Project Population Data dataset [57]. By using a machine learning approach that decomposes the population size into 100 × 100 m grid cells, it generates data on the spatial distribution of the global population from 2000–2021 utilizing the relationship between population density and a series of geospatial covariate layers.

Croplands data have been derived from MCD12Q1.006 MODIS Land Cover Type Yearly Global 500 m (MCD12Q1 V6) [58], which has a spatial resolution of 0.5 km. This dataset contains global land cover types for 2001–2020 and is based on MODIS Terra and Aqua reflectance data derived from a supervised classification.

Details of the data source for this article can be found in Supplementary Materials Table S1.

2.3. Data Processing

2.3.1. Hydrological Connectivity Index

According to the landscape connectivity theory (Figure 2), the integral index of connectivity (IIC) is used to evaluate the hydrological connectivity of BLB using Conefor Sensinode 2.6 and ArcGIS 10.2 software [59,60]. The interannual hydrological connectivity (Yearly-IIC) is calculated based on the permanent water patches in JRC-Yearly datasets, and the seasonal hydrological connectivity (Monthly-IIC) is calculated using the water patches in JRC-Monthly datasets. The interannual variability of hydrological connectivity (dIIC) serves as an index to identify the significant patches of water [22]. The threshold value for Conefor Sensinode 2.6 is determined in Supplementary Materials Text S1 and Supplementary Materials Figure S5.

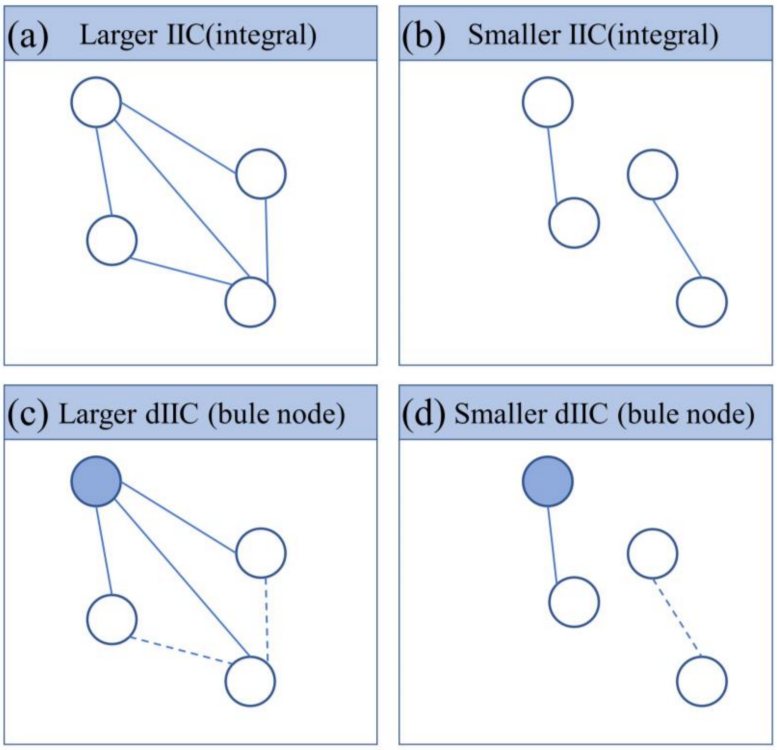

Figure 2. Different cases illustrating these two connectivity indexes. (**a**) Larger IIC: any two nodes are connecting. (**b**) Smaller IIC: pairwise connecting. (**c**) Larger dIIC for bule node: key node. (**d**) Smaller dIIC for bule node: non-key node.

Calculation of hydrological connectivity index. The integral index of connectivity (IIC) value is used to assess complex traffic topological networks, which is widely applied in the evaluation of landscape connectivity [22,61–63]. Since the index is highly sensitive to connectivity, it has also been widely used in previous studies on hydrological connectivity [22,64–66]. Therefore, IIC and dIIC are used to assess the dynamics of interannual hydrological connectivity dynamics of the BLB from 1990 to 2019 and the seasonal hydrological connectivity dynamics from 2000 to 2019 for April to October, respectively.

The IIC indicates the integral index of connectivity of the basin which is based on a binary connectivity model, indicating direct connectivity or disconnection and intuitive structural connectivity between two patches. The higher the connectivity of the study area, the higher the IIC value. The connectivity index is calculated as:

$$IIC = \frac{\sum_{i=1}^{n}\sum_{j=1}^{n}\frac{a_i \times a_j}{1+nl_{ij}}}{A_L^2} = \frac{\sum_{i=1}^{n}\sum_{j=1}^{n} a_i \times a_j \times P_{ij}^*}{A_L^2},\ (0 \le IIC \le 1) \quad (1)$$

where, n is the total number of water patches; a_i and a_j represent the area of patch i and j, respectively; nl_{ij} denotes the number of links in the shortest path between patch i and j; and A_L the area of the BLB. P_{ij}^* is the maximum multiplication probability of all possible paths between patches i and j. $P_{ij}^* = 0$ means that the two patches are completely isolated from each other. The values of IIC range from 0 to 1: when IIC = 0, there is no connection between patches; when IIC = 1, the whole landscape is actually one habitat patch. Meanwhile, in order to analyze the relationship between hydrological connectivity and water-related environment, we divided the years into high hydrological connectivity years (i.e., IIC is above the mean value) and low hydrological connectivity years (i.e., IIC is above the mean value) from 1990 to 2019.

Although, the IIC can assess the overall degree of hydrological connectivity, it lacks the ability to assess the importance of individual water patches [67]. Therefore, to identify

the importance of specific patches in the BLB and better support water conservation, the contribution of each node to the overall index was measured by removing each specific node and recalculating the IIC [22] to take into account the percentage loss. The calculation is as follows:

$$dIIC = \frac{IIC - IIC'}{IIC} \times 10 \quad (2)$$

where, IIC and $dIIC'$ correspond to the IIC value before and after the removal of a certain patch, respectively.

The Jenks natural breakpoint method [68] has been used to classify the important index of water patches for each year, and the *dIIC* is classified in six levels as unimportant (I. 0~0.99), low importance (II. 1~4.99), medium importance (III. 5~9.99), high importance (IV. 10~14.99), higher importance (V. 15~19.00) and highest importance (VI. 20~100). Based on the grading results of *dIIC*, the image maps of each year are superimposed by ArcGIS10.2 software raster calculator and classified into five categories, which are less important (importance index fluctuates between gradient I and II), important (importance index fluctuates between gradient II and III), more important (importance index fluctuates between gradient III and IV), very important (importance index fluctuates between gradient IV and V), and most important (importance index is between gradient V and VI).

2.3.2. Statistical Analysis

For discussing the effect of water abundance and depletion patterns on interannual and seasonal hydrological connectivity, based on the runoff data of the Kaidu River outlet, the years were classified into wet year, dry year, and normal year according to the typical year method (Table S2).

Trend analysis was performed using Sen's slope estimator and Pearson correlation in this study. Sen's slope estimator is often used in trend analysis of long time series data as a robust non-parametric statistical method of trend calculation that is computationally efficient and insensitive to measurement errors and outliers [69]. Pearson correlation was used to analyze the relationship between two different factors. Standard deviation (SD) and coefficient of variation (CV) were used to characterize the data's degree of dispersion.

The multiple stepwise regression model (MSRM) is used to quantify the effects of climate factors and human activities on *IIC* [70,71]. Slope > 0 is defined as positive correlation and slope < 0 is defined as negative correlation (95% confidence level). The MSRM equation is shown below:

$$IIC = aX1 + bX2 + cX3 + dX4 + eX5 + k \quad (3)$$

where, $X1$ is the total annual precipitation (mm), $X2$ is the average annual temperature (°C), $X3$ is the total annual actual evapotranspiration (mm), $X4$ is the croplands area (km^2), $X5$ is the average annual total population (person), and k is a constant.

3. Results

3.1. Characteristics of Multi-Scale Changes in Hydrological Connectivity

3.1.1. Inter-Annual Variation Characteristics of Hydrological Connectivity

The hydrological connectivity of the BLB basin in the past 30 years is low overall, with an annual average yearly-IIC index of only 0.169. In addition, three obvious fluctuating trends have emerged (Figure 3a) in three distinct corresponding periods. First, the yearly-IIC index increased at 0.004/yr from 1990 to 2000, giving an average yearly-IIC of 0.170. Secondly, from 2000 to 2007, it decreased at a rate of 0.008/yr, with an average yearly-IIC of 0.164, and then plunged to a 30-year low value of 0.146 in 2007, which was 13.59% lower than the average. In the third period (2007 to 2019), the yearly-IIC index increased again at 0.005/yr, with an average yearly-IIC of 0.173, which is the highest mean value among the three periods. It reached a maximum in 2018 of up to 0.203, which is 19.68% higher than the yearly mean value.

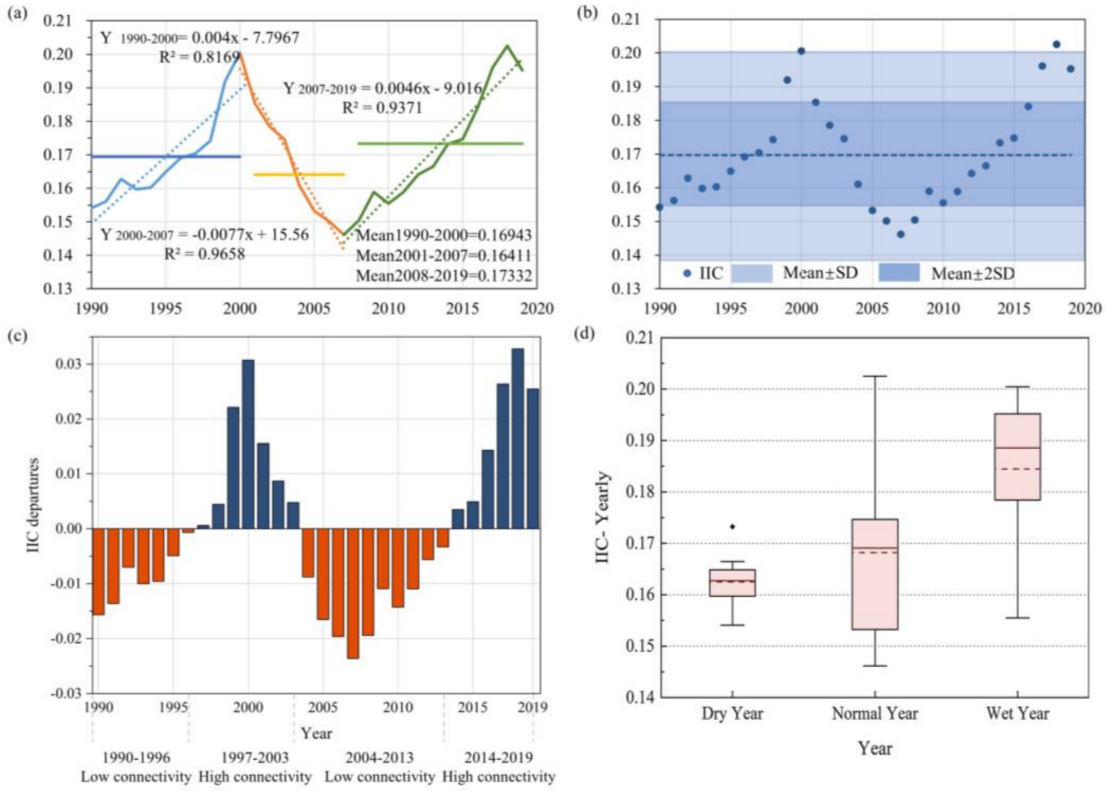

Figure 3. (**a**) Time series, trends, and staged changes of yearly-IIC of the Bosten Lake Basin from 1990–2019; (**b**) The discrete situation of IIC in the Bosten Lake Basin from 1990–2019; (**c**) IIC departures in the Bosten Lake Basin, 1990–2019, based on the average of 30-year period; (**d**) the distribution of yearly-IIC index in different years. The top and bottom of boxes represent the 75th and 25th percentiles, respectively, while the top and bottom whiskers represent the 90th and 10th percentiles, respectively. Solid red lines in the boxes are median values and dotted red lines represent mean value.

Yearly-IIC in BLB has four phases of fluctuation with surpluses and deficits in the range of ±0.03 over the last 30 years (Figure 3c). The yearly-IIC shows two high value phases (1997–2003, 2014–2019) and two low value phases (1990–1996, 2004–2013). In 1990–1996 and 2004–2013, the yearly-IIC index was lower than the 30-year average value, and the average deficit was −0.114. These two periods had an average value of yearly-IIC of 0.161 and 0.156, respectively. On the other hand, 1997–2003 and 2014–2019 were above-average periods of higher hydrological connectivity. The average surplus of these two phases was 0.149, and the mean values of yearly-IIC were 0.181 and 0.191, respectively.

The hydrological connectivity of the BLB has obvious spatial heterogeneity. The annual average yearly-IIC of KDH, KKH and KQH are 0.021, 0.032 and 0, respectively (Supplementary Figure S2). The yearly-IIC of KQH is almost zero, which is due to the prominent disconnection of the Konqi River channel [72] and serious desertification downstream, which resulted in few and scattered patches of water. The average annual IIC of KKH is higher than that of KDH and less discrete, which is mainly because KDH is a high-altitude mountainous area with unstable connectivity of water patches and is vulnerable to climate change factors, while KKH is an oasis area with more stable and higher connectivity of water patches under human management.

Figure 3d shows that the yearly-IIC is the largest in wet years (0.185) and the smallest in dry years (0.163). These data indicate that the hydrological connectivity of the basin was influenced by runoff, the hydrological connectivity was higher in wet years than in dry ones, but the variability of the yearly-IIC index is higher in wet years.

3.1.2. Seasonal Variations in Hydrological Connectivity

As shown in Figure 4a,c, there was a clear seasonal pattern in the hydrological connectivity of BLB, with an average monthly-IIC value of 0.157 from April to October. The average monthly-IIC was highest in April at 0.159 and lowest in October at 0.151. Monthly-IIC was increased at a rate of 0.0011/yr in October, while the rest of the months experienced a decreasing trend, with hydrological connectivity decreased the most (−0.0026/month) in May.

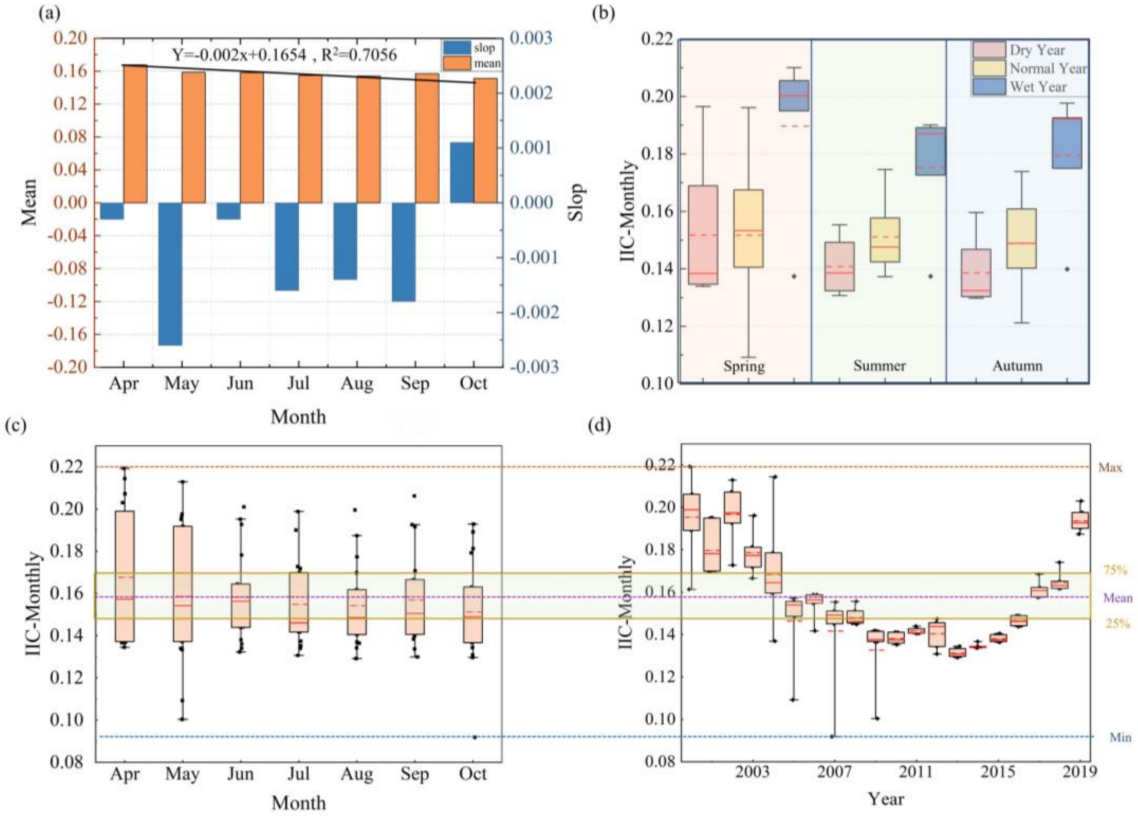

Figure 4. (**a**) Distribution of monthly-IIC; (**b**) Monthly-IIC under different seasons for different year types; (**c**) Box plot of monthly-IIC distribution from April to October in 2000 to 2019; (**d**) Monthly-IIC Distribution boxplots from April to October in 2000 to 2019. The meaning of the boxes and lines are the same with Figure 3d.

The interannual trend of monthly-IIC is similar to yearly-IIC, a 'U' shaped trend has been observed between 2000 and 2019 (Figure 4d), the data show that the monthly-IIC is lower than the yearly-IIC. To be specific, the lowest monthly-IIC value of 0.114 occurring in 2010, and the maximum value occurs in 2019 with an average monthly-IIC of 0.195. In seasonal (Figure 4b), it can be found that the monthly-IIC reached 0.160 in spring, which is higher than summer (monthly-IIC = 0.155) and autumn (monthly-IIC = 0.154). Furthermore, monthly-IIC is higher in wet years (yearly-IIC = 0.182) than in dry years (yearly-IIC = 0.144). The highest monthly-IIC occurred in the spring during the wet period (monthly-IIC = 0.190) and the lowest in the fall during the dry period (monthly-IIC = 0.139).

The monthly-IIC in the BLB is higher in the wet period than that in the dry, and higher in spring than in summer and autumn. The reason for this phenomenon may be that with the increase in temperature during the year, the water flux in the basin gets larger and vegetation grows vigorously, leading to an increase in evapotranspiration and soil evaporation, which may in turn reduce the hydrological connectivity.

3.1.3. Identification of Key Nodes in Hydrological Connectivity

As shown in Figure 5, the key nodes of hydrological connectivity BLB were mainly distributed around the Bosten Lake and the upper reaches of the Kaidu River. The dIIC value of the Bosten Lake is always more than 99, which is the largest hydrological connectivity node in the BLB. The Bosten Lake is the central node of the water network which is of great significance to the regional ecological environment. The other key nodes are primarily distributed along the Kaidu River, mainly in the small Yuldus wetland and the large Yuldus wetland, with an average dIIC of 4.142. The small Yuldus wetland and the large Yuldus wetland, important biodiversity reserves in the BLB, have a particularly prominent water conservation function.

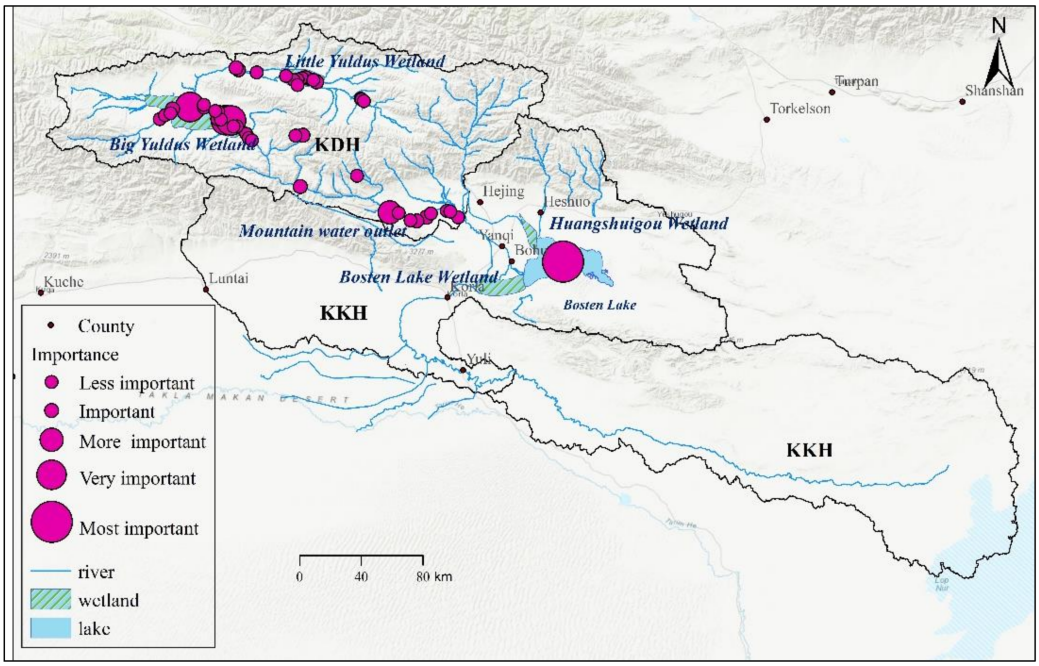

Figure 5. Distribution of key hydrological connectivity nodes in BLB.

3.2. Characteristics and Dynamics of Water Quality in the Bosten Lake

Increased hydrological connectivity will promote water exchange capacity, which will enhance the water cycle and improve the water quality. The water environmental quality of the Bosten Lake shows an overall improvement from 2001 to 2019 (Figure 6). Specifically, all indicators reveal improved quality of the Bosten Lake (except for TN), with the compliance rate of all indicators up to the Chinese Environmental Quality for Surface Water III Standard (Standard-III) (Tables S3 and S4), except for TDS, COD and TN.

Among these indices, the annual average concentration of COD is 23.41 mg/L (Figure 6b), which already exceeds the Standard III (≤20 mg/L), the attainment rate only 36.84%. The maximum value was as high as 28.68 mg/L in 2013, and only in 2006 and 2018 were the concentrations lower than 20 mg/L. The annual average concentration of TN was 0.83 mg/L, which achieved the Standard-III, and the attainment rate is 94.74%; the concentration was only exceeded in 2011, with a concentration of 1.01 mg/L (Figure 6c).

The water environmental quality of the Bosten Lake varies under different hydrological connectivity periods (Figure 7a). The annual average concentrations of DO, COD_{MN}, BOD_5, TP, TN, NH3-N and TDS in high hydrological connectivity periods are smaller than those in low periods, and the dispersion of BOD_5, TP, NH3-N and TDS has a higher degree (CV > 20%) (Table S5). However, the maximum value and the CV (CV = 9–58%) of COD_{MN}, COD, BOD_5, TN and TDS in high hydrological connectivity periods are larger than those in low hydrological connectivity periods (Figure 7a). The reason is that water movement is enhanced during high hydrological connectivity, leading to an increase in the water

quality exchange capacity, which results in fluctuating changes in water quality indices and a subsequent increase in the dispersion of water quality indicators. Among them are COD and TDS, which have the lowest rate for fulfilling the Standard III. Most of their compliance occur in high hydrological connectivity (75%). Moreover, only in one year (2011) during the low hydrological connectivity periods did TN not reach the standard.

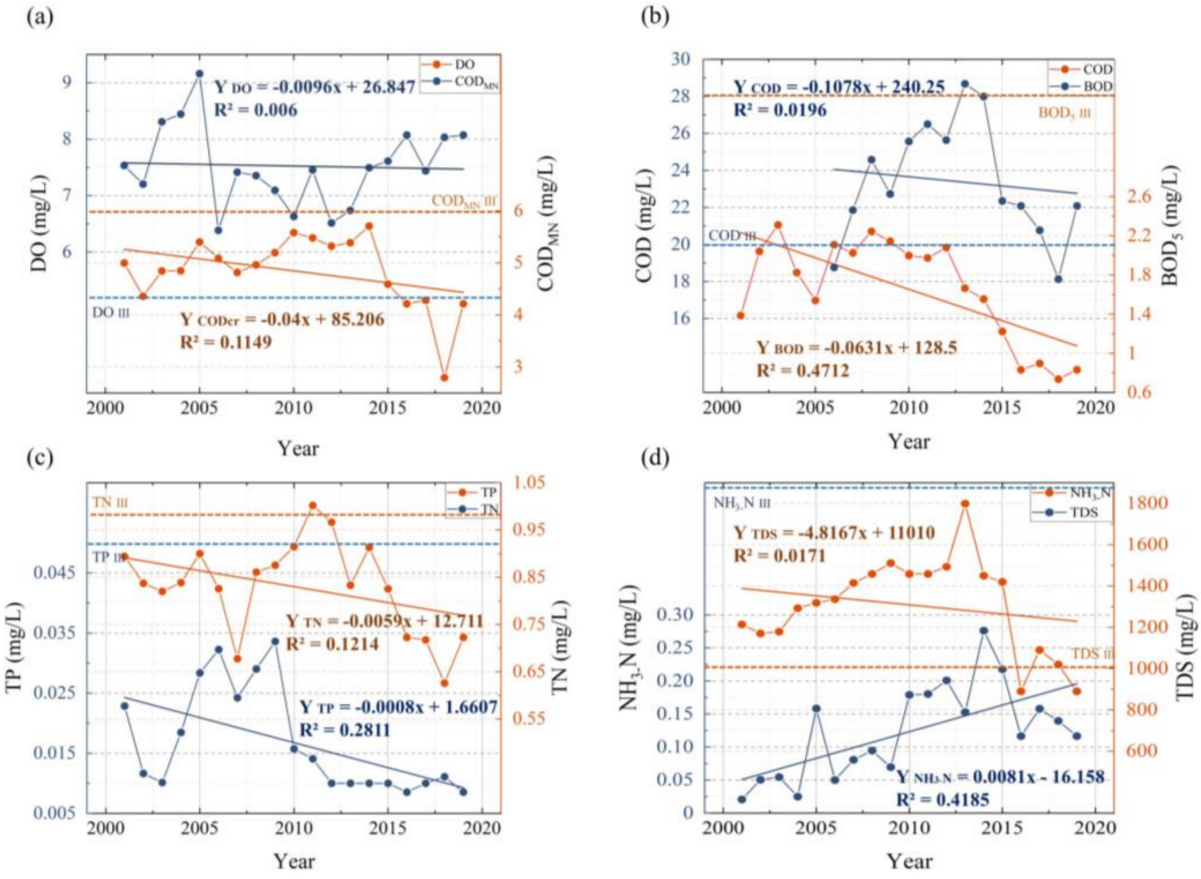

Figure 6. Interannual variation curves of eight water quality indicators, (**a**) DO and COD_{MN} (**b**) COD and BOD_5 (**c**) TP and TN (**d**) NH3-N and TDS, where the dashed lines represent the Class III standard values and freshwater standard values (TDS) of each indicator.

There are pronounced seasonal differences in the water environmental quality of the Bosten Lake. As shown in Figure 7b, concentrations of COD_{MN}, COD, BOD_5, TN, NH3-N and TDS were higher in autumn and summer than in spring, while DO concentrations were slightly higher in spring than in summer and autumn. This indicates that seasonal water quality was significantly better in the spring when hydrological connectivity was higher than in the summer and autumn when it was lower. The seasonal variation of TP was more discrete than the rest of the indicators, with CVs as high as 99%, 61%, and 80% in spring, summer, and autumn, respectively, which indicates that the higher the inter-seasonal hydrologic connectivity, the higher the variability of hydro-chemical concentration. The seasonal variation of NH3-N varies greatly (CV > 50%), while that of DO, COD, TN and TDS is less so (CV < 20%). From these data, we can see that the water quality of the Bosten Lake during high hydrological connectivity periods is better than during lower hydrological connectivity periods. However, the degree of dispersion is higher, and the seasonal variations in hydrological connectivity majorly impact the quality of the water environment.

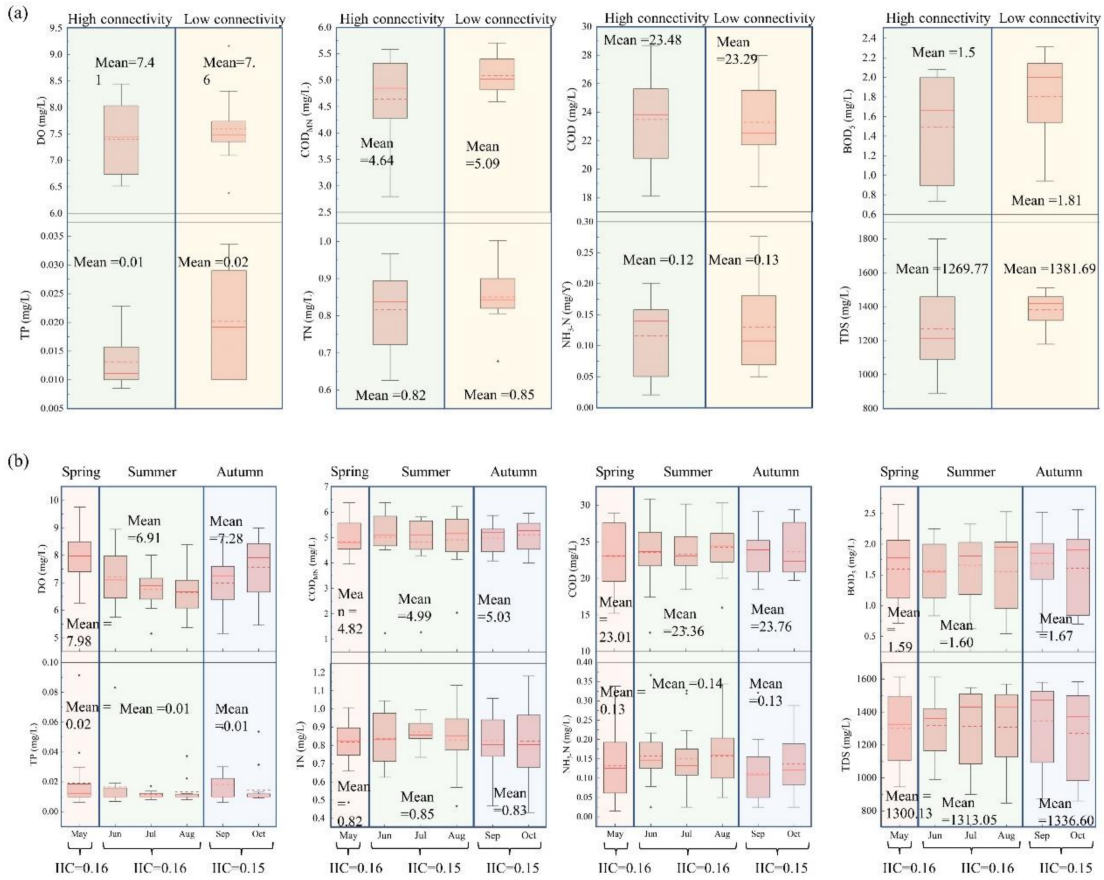

Figure 7. (**a**) Box line diagrams of 8 water quality indicators during high connectivity (green) and low connectivity (yellow) periods, respectively, dots represent the average concentration of each indicator per year; (**b**) Boxplots of 8 water quality indicators during May to October, respectively, where May is spring (red), June–August is summer (green), and September–October is autumn (blue). The meaning of the boxes and lines are the same with Figure 3d, dots represent the average concentration of each indicator per mounth.

3.3. Hydrological Connectivity and Its Water-Related Environmental Relationship

3.3.1. Anthropogenic and Climatic Drivers for IIC Dynamics

The results of the multi-step regression model used to quantify the effects of climate change and human activities on hydrological connectivity in the BLB are shown in Table S6. IIC is significantly and positively correlated with precipitation (PREC) ($p < 0.05$) and Population (POP) ($p < 0.05$). With the increase of PREC, water patch area of the basin increases, which obviously resulted in an increase in the inter-patch connectivity. As the regional population increases, the government has implemented a series of water projects and management measures (Table S7) in order to achieve sustainable water resources in the region, which may contribute to a positive correlation between population and hydrological connectivity. Simultaneously, IIC is significantly negatively correlated with actual evapotranspiration (ETa) ($p < 0.05$) and cropland ($p < 0.05$), which is also attributed to the increase in water consumption, decrease in water patch area and increase in fragmentation. The absolute value of the correlation coefficient between ETa and IIC is greater than the other indexes (Table S6), which indicates that the connectivity of water patches is mainly negatively influenced by ETa in BLB, which is different from the humid area [73–75]. The water resources in inland river basins in arid zones are formed in the mountainous areas, and precipitation in plains, which is almost not hydrologically significant, is too subtle to recharge the streamflow. Temperature (TEM) is negatively correlated with IIC, but not statistically significant.

3.3.2. Relationship between Water Quality and Hydrological Characteristics

To examine the interactions between hydrological related characteristics and hydrochemistry, a correlation study has been conducted in this paper (Figure 8). The results show that COD_{MN}, BOD_5, TP, TN, and TDS are significantly negatively correlated with IIC ($p \leq 0.05$), while DO is significantly positively correlated with IIC. The results indicated that the increase in hydrological connectivity improves water quality. At the same time, the area of total water body (TWA) and the area of the Bosten Lake area (BLA) have significant negative correlations ($p \leq 0.05$) with COD_{MN}, BOD_5 and TP, whereas the Bosten Lake level (BLL) has significant positive correlations ($p \leq 0.05$) with COD_{MN}, COD, BOD_5, TN and TDS, indicating that hydrological connectivity increases with increases in watershed area and lake level, thus improving the water environment quality.

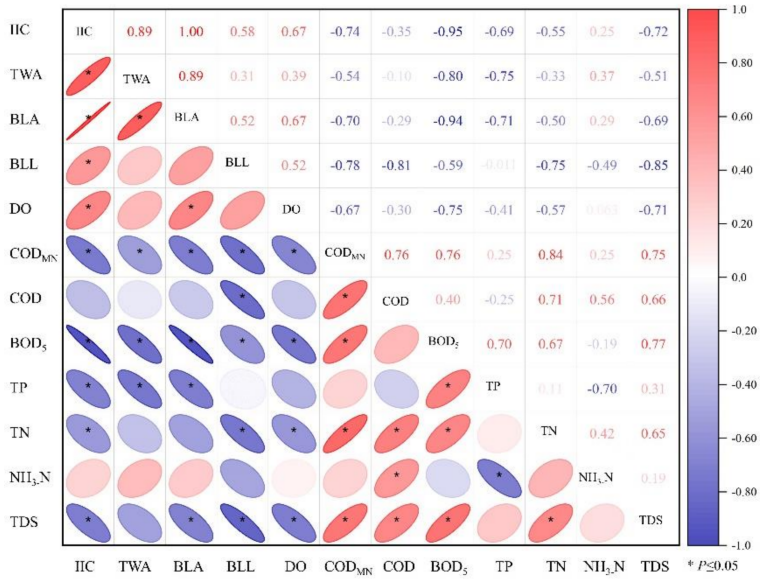

Figure 8. Correlation test of each index. IIC: integral index of connectivity; TWA: total water area; BLA: Bosten Lake area; BLL: Bosten Lake level.

Overall, there is a strong correlation between the water quality of the water environment and the hydrological characteristics. The results show that DO has a very strong positive correlation with IIC and the Bosten Lake area (BLA), ($|r| > 0.6$, $p \leq 0.05$); COD_{MN} has a very strong negative correlation with IIC, BLA and the Bosten Lake level (BLL) ($|r| > 0.6$, $p \leq 0.05$); BOD5 and TP have a very strong negative correlation with IIC, total water area (TWA) and BLA, ($|r| > 0.6$, $p \leq 0.05$); TN has a very strong negative correlation with BLL ($|r| > 0.6$, $p \leq 0.05$); TDS has a very strong negative correlation with IIC, BLA and BLL ($|r| > 0.6$, $p \leq 0.05$); and TDS has a very strong negative correlation with IIC, BLA and BLL ($|r| > 0.6$, $p \leq 0.05$). Furthermore, the results indicate that there is a strong negative correlation between TDS and IIC, and between BLA and BLL ($|r| > 0.6$, $p \leq 0.05$). This shows that the quality of the water environment will be effectively improved with increases in hydrological connectivity and water body area.

The changes and interactions between water environmental quality indicators are more complex, as shown by the significant negative correlations between DO and COD_{MN}, BOD_5, TN, TDS ($p \leq 0.05$) and negative correlations with COD and TP. The correlations with NH3-N are weak and statistically insignificant. COD_{MN} has a strong positive correlation with COD, BOD_5, TN, and TDS ($|r| > 0.6$, $p \leq 0.05$); COD has a strong positive correlation with TN, NH3-N, and TDS ($p \leq 0.05$); BOD_5 has a strong positive correlation with TP, TN, and TDS ($|r| > 0.6$, $p \leq 0.05$); and TN has a strong positive correlation with TDS ($|r| > 0.6$, $p \leq 0.05$). This phenomenon indicates that the increase in DO has a positive effect on the self-cleaning ability of the water environment. All the other water quality indicators show a

synergistic effect, such that when one water quality indicator starts to deteriorate, it causes the deterioration of other indicators as well.

4. Discussion

4.1. Anthropogenic and Climatic Drivers for Hydrological Connectivity Dynamics

Previous studies [73,75] have demonstrated that hydraulic measures such as river dredging and land use changes are the main drivers of hydrological connectivity changes. According to the statistics (Figure S3), the population and cropland in BLB increased continuously from 2001 to 2019, which likewise increased water consumption and affected terrestrial water storage [76]. This, in turn, had an impact on hydrological connectivity. Table S7 shows that most of the BLB channels have been dredged after 1990, and that several artificial channels have been built since 2000 to satisfy the increasing irrigation demand. The construction of these channels has increased the flow paths and significantly improved the possibility of water system connectivity.

Ecological water conveyance, as an effective measure to restore and protect the natural vegetation and water environment in inland river basins, is commonly used in northwest China [76–78]. Around 2010, several water system connectivity projects and hydraulic facilities were carried out in the BLB, including artificial dredging and construction channels and water transfer projects. All these hydraulic measures have effectively increased the water system connectivity in the basin, and improved the fractal structure of the water system and artificial water system connectivity. It has enabled the basin to achieve supplementary water resources and boost the complementary water resources between river-lake and reservoir. These water management measures have enhanced of the exchange of water and matter within and outside the water system, leading to an improvement of the carrying capacity of water resources in the basin, and an increase in the stability of the water system network. In cases where protective behaviors are stronger than destructive behaviors, the hydrological connectivity of the basin will improve. Otherwise, the connectivity will be reduced. Therefore, regulating all types of water use activities and construction projects in inland river basins in arid zones is essential, which can improve the structure and pattern of hydrological connectivity, as well as the function and connectivity of river and lake systems.

Our results show that the increase in hydrological connectivity caused by precipitation and temperature is not significant in the arid zone. The increase in TMP accelerate glacier melt, which led to an increase in runoff and hydrological connectivity to some extent. In contrast, ETa has a negative impact on the watershed, which will reduce hydrological connectivity.

Beel's [78] argued that the increase in river function in summer and autumn in the Arctic highlands could increase terrestrial hydrological connectivity. However, we find that the seasonal variation in hydrological connectivity is higher in spring than in summer and autumn (Figure 4), as surface water in the arid inland river basins is mainly influenced by ETa. Hydrological connectivity is higher in spring with snowmelt, but as temperature rises, vegetation grows and regional evapotranspiration increases, the water flux becomes larger, resulting in an amount of water surface evapotranspiration and the connectivity of water patches is reduced.

4.2. Ecological and Hydrochemical Characteristics of Lakes in Response to Hydrological Characteristics

As illustrated in Figure 8, there is a strong positive relationship among hydrological connectivity, water body area, lake area and water level. When the water level of the lake increases, the water area likewise increases, and as total water body area increases, there is an obvious increase in hydrological connectivity. As the largest throughput freshwater lake in China, the Bosten Lake is a broad and shallow basin, with rises in water level, the surface area of the lake will increase, isolated patches of water will be connected with each other, thus increasing hydrological connectivity [79,80]. However, as the lake area increases, the

evaporation of water from the lake surface will increase, as well as the ineffective water loss of the lake. While when the water level is too low, the exposed surface area increases, and the large area of exposed fine sand of the lake basin, that is in the northwest and south shore of the lake, will directly aggravate the wind and dust storms around the Bosten Lake, and affect the environment suitable for people to live. Therefore, there may be an inverted U-shaped relationship between hydrological connectivity, lake level, water area, and ecology that is similar to an environmental Kuznets curve [40].

As the biggest inland freshwater lake in China, the largest hydrologically connected node in the basin (Figure 5), the soil salinization in the surrounding areas is seriously overloaded with nutrients. Despite the local government implementing a series of water conservation policies and projects, it still has not been able to change the fact that the Bosten Lake is gradually transforming into a micro-salt lake (TDS > 1000 mg/L) [2,28,81]. The continued increase of salinity not only adversely affects the lake ecosystem, regional ecology and water resources utilization, but also has become a serious environmental problem in the lake itself [48]. Our study found that between 1990 and 2019, the Bosten Lake had met freshwater standards for TDS concentrations twice only—in 2016 and 2019 (TDS $\leq$ 1000 mg/L) (Figure 6d).

From 2016 to 2020, in response to the problems of broken streams and deteriorating water environment around the Bosten Lake, along with poor water circulation and water environment quality in the northern part of the lake, three water system connection projects were implemented. A total of about 4.79×10^8 m^3 (Table S7) of water was ecologically transferred to the Bosten Lake, which provided an important basis for the improvement of the lake's water environment quality. According to the correlation test (Figure 8), TDS shows a strong negative correlation with IIC, BLA, and BLL ($|r| > 0.6$, $p \leq 0.05$). This phenomenon suggests that the hydrological connectivity, BLL and BWA play an important role in the dynamics of lake water salinity. Our results also show that from 2007 to 2014, hydrological connectivity increased (Figure 4a), while BLL decreased (Figure S1). At the same time, however, TDS also increased (Figure 6d). The correlation between TDS and BLL was greater than that between IIC and BLA based on the correlation test, indicating a more significant regulation of TDS by BLL [28,47]. This may be because as the lake level increases, the decrease in hydrochemical concentration caused by the increase in lake volume is more efficient than that of water exchange. However, the existing hydrological connectivity evaluation models lack the representation of hydrological connectivity processes, so it is difficult to reveal the kinetics of water exchange quantitatively, which will be the focus of our next research. Also, we will improve the method of assessing hydrological connectivity, which is influenced by the area of water bodies and the distance of patches.

5. Conclusions

In this study, we applied the concept of landscape connectivity and used landscape graph theory to evaluate the connectivity characteristics of water patches in BLB from 1990 to 2019, and analyzed the water quality changes in Lake Bosten over the last 20 years, emphasizing the regulation effects of hydrological connectivity on water quality. The results indicate that the hydrological connectivity of BLB is low (IIC = 0 ~ 0.2025, IIC_{MAX} = 1) and cyclical, and the hydrological connectivity is higher in oasis than mountain and desert areas. At the same time, the water resources in inland river basins in arid zones are formed in mountainous areas, and precipitation in plains is almost not hydrologically significant. Temperature (TEM) is negatively correlated with IIC, but not statistically significant. Furthermore, seasonal hydrological connectivity is highest in spring and lowest in autumn.

From 2000 to 2019, the water environmental quality of the lake gradually improved, and the pollution indicators mainly related to TDS, COD and TN. Most importantly, there is a significant negative correlation between COD_{MN}, BOD_5, TP, TN, and TDS and IIC ($p \leq 0.05$), and DO was significantly positively correlated with IIC, and the annual average concentrations of COD_{MN}, BOD_5, TP, TN, NH3-N and TDS in high hydrological

connectivity periods are smaller than those in low periods, and most of their compliance periods occur during high hydrological connectivity (75%), it can be found that hydrological connectivity plays a key role in improving the water quality of the Bosten Lake, the minimum value have occurred during periods of high hydrological connectivity.

Supplementary Materials: The following supporting information can be downloaded at: https://www.mdpi.com/article/10.3390/rs14194977/s1, Text S1. Selection of hydrological connectivity thresholds, Text S2. Characteristics of water body changes in the BLB, Text S3. Water quality change characteristics from 2001–2019, Figure S1. Change trend of Bosten lake water area and level change from 1990 to 2019, Figure S2. Time series and trends of yearly IIC from 1990–2019 of each sub-basin, Figure S3. Arable land area and population change of BLB, Figure S4. Temporal and spatial variations of PREC, ETa and TMP and their significance tests. Black dots represent passing the $p < 0.05$ test, Figure S5. Variation of IIC at different distance thresholds, Figure S6. 1990–2019 BLB (a) variations of TWA, PWA, SWA, (b) percentage of PWA and SWA, and (c) conversion between different types of water bodies, Figure S7. (a) Water area distribution in 1990, (b) water area distribution in 2019, (c) water area change from 1990 to 1996, (d) water area change from 1996 to 2000, (e) water area change from 2000 to 2005, (f) water area change from 2005 to 2010, (g) water area change from 2010 to 2015, (h) water area change from 2015 to 2019, Table S1. Details of the data source for this article, Table S2. Classification results of wet, dry and normal years from 1990 to 2019, Table S3. Chinese Environmental Quality for Surface Water III Standard(GB3838-2002), Table S4. Standard for classification of fresh and salt water, Table S5. Characteristic values of interannual variation of water quality indexes, Table S6. Multiple stepwise regression results, Table S7. Water System connectivity Project of BLB. References [82–85] are cited in Supplementary Materials.

Author Contributions: C.L. and Y.C. conceived of the original design of this paper. G.F., H.Z. and W.H. improve the structure of the paper. Z.L., Y.L. and X.W. provided comments on this paper. All authors have read and agreed to the published version of the manuscript.

Funding: This work is supported by the Natural Science Foundation of Xinjiang (2021D01D01) and the Key Research Program of the Chinese Academy of Sciences (ZDRWZS-2019-3).

Institutional Review Board Statement: Not applicable.

Informed Consent Statement: Not applicable.

Data Availability Statement: JRC Yearly Water Classification History, v1.3 and JRC Monthly Water Classification History, v1.3 are openly available via https://earthengine.google.com/ (accessed on 20 September 2021).

Conflicts of Interest: The authors declare that they have no known competing financial interests or personal relationships that could have appeared to influence the work reported in this paper.

References

1. Boulton, A.J.; Rolls, R.J.; Jaeger, K.L.; Datry, T. Chapter 2.3—Hydrological Connectivity in Intermittent Rivers and Ephemeral Streams. In *Intermittent Rivers and Ephemeral Streams*; Datry, T., Bonada, N., Boulton, A., Eds.; Academic Press: Cambridge, MA, USA, 2017; pp. 79–108; ISBN 978-0-12-803835-2.
2. Hassani, A.; Azapagic, A.; Shokri, N. Global Predictions of Primary Soil Salinization under Changing Climate in the 21st Century. *Nat. Commun.* **2021**, *12*, 6663. [CrossRef] [PubMed]
3. Keeley, A.T.H.; Beier, P.; Jenness, J.S. Connectivity Metrics for Conservation Planning and Monitoring. *Biol. Conserv.* **2021**, *255*, 109008. [CrossRef]
4. Kraaijenbrink, P.D.A.; Stigter, E.E.; Yao, T.; Immerzeel, W.W. Climate Change Decisive for Asia's Snow Meltwater Supply. *Nat. Clim. Chang.* **2021**, *11*, 591–597. [CrossRef]
5. Osman, M.B.; Tierney, J.E.; Zhu, J.; Tardif, R.; Hakim, G.J.; King, J.; Poulsen, C.J. Globally Resolved Surface Temperatures since the Last Glacial Maximum. *Nature* **2021**, *599*, 239–244. [CrossRef] [PubMed]
6. Yao, J.; Chen, Y.; Guan, X.; Zhao, Y.; Chen, J.; Mao, W. Recent Climate and Hydrological Changes in a Mountain–Basin System in Xinjiang, China. *Earth-Sci. Rev.* **2022**, *226*, 103957. [CrossRef]
7. Messager, M.L.; Lehner, B.; Cockburn, C.; Lamouroux, N.; Pella, H.; Snelder, T.; Tockner, K.; Trautmann, T.; Watt, C.; Datry, T. Global Prevalence of Non-Perennial Rivers and Streams. *Nature* **2021**, *594*, 391–397. [CrossRef]
8. Grill, G.; Lehner, B.; Thieme, M.; Geenen, B.; Tickner, D.; Antonelli, F.; Babu, S.; Borrelli, P.; Cheng, L.; Crochetiere, H.; et al. Mapping the World's Free-Flowing Rivers. *Nature* **2019**, *569*, 215–221. [CrossRef]

9. Cooley, S.W.; Ryan, J.C.; Smith, L.C. Human Alteration of Global Surface Water Storage Variability. *Nature* **2021**, *591*, 78–81. [CrossRef]
10. Schmitt, R.J.P.; Bizzi, S.; Castelletti, A.; Kondolf, G.M. Improved Trade-Offs of Hydropower and Sand Connectivity by Strategic Dam Planning in the Mekong. *Nat. Sustain.* **2018**, *1*, 96–104. [CrossRef]
11. Tan, Z.; Li, Y.; Zhang, Q.; Liu, X.; Song, Y.; Xue, C.; Lu, J. Assessing Effective Hydrological Connectivity for Floodplains with a Framework Integrating Habitat Suitability and Sediment Suspension Behavior. *Water Res.* **2021**, *201*, 117253. [CrossRef]
12. Belletti, B.; Garcia de Leaniz, C.; Jones, J.; Bizzi, S.; Börger, L.; Segura, G.; Castelletti, A.; van de Bund, W.; Aarestrup, K.; Barry, J.; et al. More than One Million Barriers Fragment Europe's Rivers. *Nature* **2020**, *588*, 436–441. [CrossRef] [PubMed]
13. Lynch, L.M.; Sutfin, N.A.; Fegel, T.S.; Boot, C.M.; Covino, T.P.; Wallenstein, M.D. River Channel Connectivity Shifts Metabolite Composition and Dissolved Organic Matter Chemistry. *Nat. Commun.* **2019**, *10*, 459. [CrossRef] [PubMed]
14. Ali, G.; English, C. Phytoplankton Blooms in Lake Winnipeg Linked to Selective Water-Gatekeeper Connectivity. *Sci. Rep.* **2019**, *9*, 8395. [CrossRef] [PubMed]
15. Anderson, E.P.; Jenkins, C.N.; Heilpern, S.; Maldonado-Ocampo, J.A.; Carvajal-Vallejos, F.M.; Encalada, A.C.; Rivadeneira, J.F.; Hidalgo, M.; Cañas, C.M.; Ortega, H.; et al. Fragmentation of Andes-to-Amazon Connectivity by Hydropower Dams. *Sci. Adv.* **2018**, *4*, eaao1642. [CrossRef] [PubMed]
16. Lam, N.S.-N.; Cheng, W.; Zou, L.; Cai, H. Effects of Landscape Fragmentation on Land Loss. *Remote Sens. Environ.* **2018**, *209*, 253–262. [CrossRef]
17. Bracken, L.J.; Croke, J. The Concept of Hydrological Connectivity and Its Contribution to Understanding Runoff-Dominated Geomorphic Systems. *Hydrol. Processes* **2007**, *21*, 1749–1763. [CrossRef]
18. Pringle, C. What Is Hydrologic Connectivity and Why Is It Ecologically Important? *Hydrol. Processes* **2003**, *17*, 2685–2689. [CrossRef]
19. Wohl, E.; Brierley, G.; Cadol, D.; Coulthard, T.J.; Covino, T.; Fryirs, K.A.; Grant, G.; Hilton, R.G.; Lane, S.N.; Magilligan, F.J.; et al. Connectivity as an Emergent Property of Geomorphic Systems. *Earth Surf. Processes Landf.* **2019**, *44*, 4–26. [CrossRef]
20. Coulthard, T.J.; Van De Wiel, M.J. Modelling Long Term Basin Scale Sediment Connectivity, Driven by Spatial Land Use Changes. *Geomorphology* **2017**, *277*, 265–281. [CrossRef]
21. Jahanishakib, F.; Salmanmahiny, A.; Mirkarimi, S.H.; Poodat, F. Hydrological Connectivity Assessment of Landscape Ecological Network to Mitigate Development Impacts. *J. Environ. Manag.* **2021**, *296*, 113169. [CrossRef]
22. Sun, C.; Chen, L.; Zhu, H.; Xie, H.; Qi, S.; Shen, Z. New Framework for Natural-Artificial Transport Paths and Hydrological Connectivity Analysis in an Agriculture-Intensive Catchment. *Water Res.* **2021**, *196*, 117015. [CrossRef] [PubMed]
23. Liu, J.; Engel, B.A.; Dai, L.; Wang, Y.; Wu, Y.; Yan, G.; Cong, L.; Zhai, J.; Zhang, Z.; Zhang, M. Capturing Hydrological Connectivity Structure of Wetlands with Indices Based on Graph Theory: A Case Study in Yellow River Delta. *J. Clean. Prod.* **2019**, *239*, 118059. [CrossRef]
24. Yu, Z.; Wang, Q.; Xu, Y.; Lu, M.; Lin, Z.; Gao, B. Dynamic Impacts of Changes in River Structure and Connectivity on Water Quality under Urbanization in the Yangtze River Delta Plain. *Ecol. Indic.* **2022**, *135*, 108582. [CrossRef]
25. Li, Y.; Zhang, Q.; Cai, Y.; Tan, Z.; Wu, H.; Liu, X.; Yao, J. Hydrodynamic Investigation of Surface Hydrological Connectivity and Its Effects on the Water Quality of Seasonal Lakes: Insights from a Complex Floodplain Setting (Poyang Lake, China). *Sci. Total Environ.* **2019**, *660*, 245–259. [CrossRef] [PubMed]
26. Goodwell, A.E.; Kumar, P.; Fellows, A.W.; Flerchinger, G.N. Dynamic Process Connectivity Explains Ecohydrologic Responses to Rainfall Pulses and Drought. *Proc. Natl. Acad. Sci. USA* **2018**, *115*, E8604–E8613. [CrossRef]
27. Deng, X. Correlations between Water Quality and the Structure and Connectivity of the River Network in the Southern Jiangsu Plain, Eastern China. *Sci. Total Environ.* **2019**, *664*, 583–594. [CrossRef]
28. Zhou, L.; Zhou, Y.; Hu, Y.; Cai, J.; Bai, C.; Shao, K.; Gao, G.; Zhang, Y.; Jeppesen, E.; Tang, X. Hydraulic Connectivity and Evaporation Control the Water Quality and Sources of Chromophoric Dissolved Organic Matter in Lake Bosten in Arid Northwest China. *Chemosphere* **2017**, *188*, 608–617. [CrossRef]
29. Yu, X.; Hawley-Howard, J.; Pitt, A.L.; Wang, J.-J.; Baldwin, R.F.; Chow, A.T. Water Quality of Small Seasonal Wetlands in the Piedmont Ecoregion, South Carolina, USA: Effects of Land Use and Hydrological Connectivity. *Water Res.* **2015**, *73*, 98–108. [CrossRef]
30. Peršić, V.; Čerba, D.; Bogut, I.; Horvatić, J. Trophic State and Water Quality in the Danube Floodplain Lake (Kopački Rit Nature Park, Croatia) in Relation to Hydrological Connectivity. In *Eutrophication: Causes, Consequences and Control*; Ansari, A.A., Singh Gill, S., Lanza, G.R., Rast, W., Eds.; Springer Netherlands: Dordrecht, The Netherlands, 2011; pp. 109–129. ISBN 978-90-481-9625-8.
31. Maes, D.; Van Dyck, H. Climate-Driven Range Expansion through Anthropogenic Landscapes: Landscape Connectivity Matters. *Glob. Change Biol.* **2022**, *28*, 4920–4922. [CrossRef]
32. Damschen, E.I.; Brudvig, L.A.; Burt, M.A.; Fletcher, R.J.; Haddad, N.M.; Levey, D.J.; Orrock, J.L.; Resasco, J.; Tewksbury, J.J. Ongoing Accumulation of Plant Diversity through Habitat Connectivity in an 18-Year Experiment. *Science* **2019**, *365*, 1478–1480. [CrossRef]
33. Saco, P.M.; Rodríguez, J.F.; Moreno-de las Heras, M.; Keesstra, S.; Azadi, S.; Sandi, S.; Baartman, J.; Rodrigo-Comino, J.; Rossi, M.J. Using Hydrological Connectivity to Detect Transitions and Degradation Thresholds: Applications to Dryland Systems. *Catena* **2020**, *186*, 104354. [CrossRef]

34. McLaughlin, D.L.; Diamond, J.S.; Quintero, C.; Heffernan, J.; Cohen, M.J. Wetland Connectivity Thresholds and Flow Dynamics from Stage Measurements. *Water Resour. Res.* **2019**, *55*, 6018–6032. [CrossRef]
35. Okin, G.S.; Sala, O.E.; Vivoni, E.R.; Zhang, J.; Bhattachan, A. The Interactive Role of Wind and Water in Functioning of Drylands: What Does the Future Hold? *BioScience* **2018**, *68*, 670–677. [CrossRef]
36. Ryser, R.; Hirt, M.R.; Häussler, J.; Gravel, D.; Brose, U. Landscape Heterogeneity Buffers Biodiversity of Simulated Meta-Food-Webs under Global Change through Rescue and Drainage Effects. *Nat. Commun.* **2021**, *12*, 4716. [CrossRef] [PubMed]
37. Liu, J.; Engel, B.A.; Zhang, G.; Wang, Y.; Wu, Y.; Zhang, M.; Zhang, Z. Hydrological Connectivity: One of the Driving Factors of Plant Communities in the Yellow River Delta. *Ecol. Indic.* **2020**, *112*, 106150. [CrossRef]
38. Liu, Y.; Cui, B.; Du, J.; Wang, Q.; Yu, S.; Yang, W. A Method for Evaluating the Longitudinal Functional Connectivity of a River–Lake–Marsh System and Its Application in China. *Hydrol. Processes* **2020**, *34*, 5278–5297. [CrossRef]
39. Zuecco, G.; Rinderer, M.; Penna, D.; Borga, M.; van Meerveld, H.J. Quantification of Subsurface Hydrologic Connectivity in Four Headwater Catchments Using Graph Theory. *Sci. Total Environ.* **2019**, *646*, 1265–1280. [CrossRef]
40. Deng, X. Influence of Water Body Area on Water Quality in the Southern Jiangsu Plain, Eastern China. *J. Clean. Prod.* **2020**, *254*, 120136. [CrossRef]
41. Norton, A.J.; Rayner, P.J.; Wang, Y.-P.; Parazoo, N.C.; Baskaran, L.; Briggs, P.R.; Haverd, V.; Doughty, R. Hydrologic Connectivity Drives Extremes and High Variability in Vegetation Productivity across Australian Arid and Semi-Arid Ecosystems. *Remote Sens. Environ.* **2022**, *272*, 112937. [CrossRef]
42. Souza, J.; Hooke, J. Influence of Seasonal Vegetation Dynamics on Hydrological Connectivity in Tropical Drylands. *Hydrol. Processes* **2021**, *35*, e14427. [CrossRef]
43. Wu, Y.; Zhang, Y.; Dai, L.; Xie, L.; Zhao, S.; Liu, Y.; Zhang, Z. Hydrological Connectivity Improves Soil Nutrients and Root Architecture at the Soil Profile Scale in a Wetland Ecosystem. *Sci. Total Environ.* **2021**, *762*, 143162. [CrossRef] [PubMed]
44. Mainali, J.; Chang, H. Landscape and Anthropogenic Factors Affecting Spatial Patterns of Water Quality Trends in a Large River Basin, South Korea. *J. Hydrol.* **2018**, *564*, 26–40. [CrossRef]
45. Dai, X.; Zhou, Y.; Ma, W.; Zhou, L. Influence of Spatial Variation in Land-Use Patterns and Topography on Water Quality of the Rivers Inflowing to Fuxian Lake, a Large Deep Lake in the Plateau of Southwestern China. *Ecol. Eng.* **2017**, *99*, 417–428. [CrossRef]
46. Wang, Y.; Zhou, X.; Engel, B. Water Environment Carrying Capacity in Bosten Lake Basin. *J. Clean. Prod.* **2018**, *199*, 574–583. [CrossRef]
47. Yao, J.; Chen, Y.; Zhao, Y.; Yu, X. Hydroclimatic Changes of Lake Bosten in Northwest China during the Last Decades. *Sci. Rep.* **2018**, *8*, 9118. [CrossRef] [PubMed]
48. Guo, M.; Wu, W.; Zhou, X.; Chen, Y.; Li, J. Investigation of the Dramatic Changes in Lake Level of the Bosten Lake in Northwestern China. *Theor. Appl. Climatol.* **2015**, *119*, 341–351. [CrossRef]
49. Dai, J.; Tang, X.; Gao, G.; Chen, D.; Shao, K.; Cai, X.; Zhang, L. Effects of Salinity and Nutrients on Sedimentary Bacterial Communities in Oligosaline Lake Bosten, Northwestern China. *Aquat. Microb. Ecol.* **2013**, *69*, 123–134. [CrossRef]
50. Ma, L.; Abuduwaili, J.; Liu, W. Environmentally Sensitive Grain-Size Component Records and Its Response to Climatic and Anthropogenic Influences in Bosten Lake Region, China. *Sci. Rep.* **2020**, *10*, 942. [CrossRef] [PubMed]
51. Zhang, L.; Shen, T.; Cheng, Y.; Zhao, T.; Li, L.; Qi, P. Temporal and Spatial Variations in the Bacterial Community Composition in Lake Bosten, a Large, Brackish Lake in China. *Sci. Rep.* **2020**, *10*, 304. [CrossRef] [PubMed]
52. Li, N.; Kinzelbach, W.; Li, W.; Dong, X. Box Model and 1D Longitudinal Model of Flow and Transport in Bosten Lake, China. *J. Hydrol.* **2015**, *524*, 62–71. [CrossRef]
53. Pekel, J.-F.; Cottam, A.; Gorelick, N.; Belward, A.S. High-Resolution Mapping of Global Surface Water and Its Long-Term Changes. *Nature* **2016**, *540*, 418–422. [CrossRef] [PubMed]
54. Worden, J.; de Beurs, K.M.; Koch, J.; Owsley, B.C. Application of Spectral Index-Based Logistic Regression to Detect Inland Water in the South Caucasus. *Remote Sens.* **2021**, *13*, 5099. [CrossRef]
55. Xi, Y.; Peng, S.; Ciais, P.; Chen, Y. Future Impacts of Climate Change on Inland Ramsar Wetlands. *Nat. Clim. Chang.* **2021**, *11*, 45–51. [CrossRef]
56. Abatzoglou, J.T.; Dobrowski, S.Z.; Parks, S.A.; Hegewisch, K.C. TerraClimate, a High-Resolution Global Dataset of Monthly Climate and Climatic Water Balance from 1958–2015. *Sci. Data* **2018**, *5*, 170191. [CrossRef] [PubMed]
57. Tatem, A.J. WorldPop, Open Data for Spatial Demography. *Sci. Data* **2017**, *4*, 170004. [CrossRef] [PubMed]
58. Chirachawala, C.; Shrestha, S.; Babel, M.S.; Virdis, S.G.P.; Wichakul, S. Evaluation of Global Land Use/Land Cover Products for Hydrologic Simulation in the Upper Yom River Basin, Thailand. *Sci. Total Environ.* **2020**, *708*, 135148. [CrossRef] [PubMed]
59. Pascual-Hortal, L.; Saura, S. Comparison and Development of New Graph-Based Landscape Connectivity Indices: Towards the Priorization of Habitat Patches and Corridors for Conservation. *Landsc. Ecol.* **2006**, *21*, 959–967. [CrossRef]
60. Saura, S.; Torné, J. Conefor Sensinode 2.2: A Software Package for Quantifying the Importance of Habitat Patches for Landscape Connectivity. *Environ. Model. Softw.* **2009**, *24*, 135–139. [CrossRef]
61. Justeau-Allaire, D.; Vieilledent, G.; Rinck, N.; Vismara, P.; Lorca, X.; Birnbaum, P. Constrained Optimization of Landscape Indices in Conservation Planning to Support Ecological Restoration in New Caledonia. *J. Appl. Ecol.* **2021**, *58*, 744–754. [CrossRef]
62. Guo, X.; Zhang, X.; Du, S.; Li, C.; Siu, Y.L.; Rong, Y.; Yang, H. The Impact of Onshore Wind Power Projects on Ecological Corridors and Landscape Connectivity in Shanxi, China. *J. Clean. Prod.* **2020**, *254*, 120075. [CrossRef]

63. Babí Almenar, J.; Bolowich, A.; Elliot, T.; Geneletti, D.; Sonnemann, G.; Rugani, B. Assessing Habitat Loss, Fragmentation and Ecological Connectivity in Luxembourg to Support Spatial Planning. *Landsc. Urban Plan.* **2019**, *189*, 335–351. [CrossRef]
64. Heckmann, T.; Cavalli, M.; Cerdan, O.; Foerster, S.; Javaux, M.; Lode, E.; Smetanová, A.; Vericat, D.; Brardinoni, F. Indices of Sediment Connectivity: Opportunities, Challenges and Limitations. *Earth-Sci. Rev.* **2018**, *187*, 77–108. [CrossRef]
65. Lehotský, M.; Rusnák, M.; Kidová, A.; Dudžák, J. Multitemporal Assessment of Coarse Sediment Connectivity along a Braided-Wandering River. *Land Degrad. Dev.* **2018**, *29*, 1249–1261. [CrossRef]
66. Erős, T.; Schmera, D.; Schick, R.S. Network Thinking in Riverscape Conservation—A Graph-Based Approach. *Biol. Conserv.* **2011**, *144*, 184–192. [CrossRef]
67. Ribeiro, R.; Carretero, M.A.; Sillero, N.; Alarcos, G.; Ortiz-Santaliestra, M.; Lizana, M.; Llorente, G.A. The Pond Network: Can Structural Connectivity Reflect on (Amphibian) Biodiversity Patterns? *Landsc. Ecol.* **2011**, *26*, 673–682. [CrossRef]
68. Xie, Y.; Li, Z.; Zhu, L.; Zhou, Y.; Liu, H.; Yu, T. Dynamic Monitoring of Desertification in Response to Climatic Factors: A Case Study from the Gelintan Oasis on the Southeastern Edge of the Tengger Desert, China. *Geocarto Int.* **2021**, 1–21. [CrossRef]
69. Notarnicola, C. Hotspots of Snow Cover Changes in Global Mountain Regions over 2000–2018. *Remote Sens. Environ.* **2020**, *243*, 111781. [CrossRef]
70. Finkler, N.R.; Gücker, B.; Boëchat, I.G.; Ferreira, M.S.; Tanaka, M.O.; Cunha, D.G.F. Riparian Land Use and Hydrological Connectivity Influence Nutrient Retention in Tropical Rivers Receiving Wastewater Treatment Plant Discharge. *Front. Environ. Sci.* **2021**, *9*, 709922. [CrossRef]
71. Niu, L.; Cai, H.; Jia, L.; Luo, X.; Tao, W.; Dong, Y.; Yang, Q. Metal Pollution in the Pearl River Estuary and Implications for Estuary Management: The Influence of Hydrological Connectivity Associated with Estuarine Mixing. *Ecotoxicol. Environ. Saf.* **2021**, *225*, 112747. [CrossRef] [PubMed]
72. Fu, A.; Li, W.; Chen, Y.; Liu, Y. Suitable Oasis Scales under a Government Plan in the Kaidu-Konqi River Basin of Northwest Arid Region, China. *PeerJ* **2018**, *6*, e4943. [CrossRef] [PubMed]
73. Xia, Y.; Fang, C.; Lin, H.; Li, H.; Wu, B. Spatiotemporal Evolution of Wetland Eco-Hydrological Connectivity in the Poyang Lake Area Based on Long Time-Series Remote Sensing Images. *Remote Sens.* **2021**, *13*, 4812. [CrossRef]
74. Liu, X.; Zhang, Q.; Li, Y.; Tan, Z.; Werner, A.D. Satellite Image-Based Investigation of the Seasonal Variations in the Hydrological Connectivity of a Large Floodplain (Poyang Lake, China). *J. Hydrol.* **2020**, *585*, 124810. [CrossRef]
75. Deng, X.; Xu, Y.; Han, L.; Song, S.; Xu, G.; Xiang, J. Spatial-Temporal Changes in the Longitudinal Functional Connectivity of River Systems in the Taihu Plain, China. *J. Hydrol.* **2018**, *566*, 846–859. [CrossRef]
76. Wang, X.; Xiao, X.; Zou, Z.; Dong, J.; Qin, Y.; Doughty, R.B.; Menarguez, M.A.; Chen, B.; Wang, J.; Ye, H.; et al. Gainers and Losers of Surface and Terrestrial Water Resources in China during 1989–2016. *Nat. Commun.* **2020**, *11*, 3471. [CrossRef] [PubMed]
77. Hu, S.; Ma, R.; Sun, Z.; Ge, M.; Zeng, L.; Huang, F.; Bu, J.; Wang, Z. Determination of the Optimal Ecological Water Conveyance Volume for Vegetation Restoration in an Arid Inland River Basin, Northwestern China. *Sci. Total Environ.* **2021**, *788*, 147775. [CrossRef] [PubMed]
78. Beel, C.R.; Heslop, J.K.; Orwin, J.F.; Pope, M.A.; Schevers, A.J.; Hung, J.K.Y.; Lafrenière, M.J.; Lamoureux, S.F. Emerging Dominance of Summer Rainfall Driving High Arctic Terrestrial-Aquatic Connectivity. *Nat. Commun.* **2021**, *12*, 1448. [CrossRef]
79. Li, Z.; Sun, W.; Chen, H.; Xue, B.; Yu, J.; Tian, Z. Interannual and Seasonal Variations of Hydrological Connectivity in a Large Shallow Wetland of North China Estimated from Landsat 8 Images. *Remote Sens.* **2021**, *13*, 1214. [CrossRef]
80. Deng, X.; Xu, Y.; Han, L. Impacts of Human Activities on the Structural and Functional Connectivity of a River Network in the Taihu Plain. *Land Degrad. Dev.* **2018**, *29*, 2575–2588. [CrossRef]
81. Tang, X.; Guijuan, X.; Shao, K.; Bayartu, S.; Chen, Y.; Gao, G. Influence of Salinity on the Bacterial Community Composition in Lake Bosten, a Large Oligosaline Lake in Arid Northwestern China. *Appl. Environ. Microbiol.* **2012**, *78*, 4748–4751. [CrossRef]
82. Ariken, M.; Zhang, F.; Liu, K.; Fang, C.; Kung, H.-T. Coupling coordination analysis of urbanization and eco-environment in Yanqi Basin based on multi-source remote sensing data. *Ecol. Indic.* **2020**, *114*, 106331. [CrossRef]
83. Deng, H.; Chen, Y.; Wang, H.; Zhang, S. Climate change with elevation and its potential impact on water resources in the Tianshan Mountains, Central Asia. *Glob. Planet. Change* **2015**, *135*, 28–37. [CrossRef]
84. Fan, M.; Xu, J.; Chen, Y.; Li, W. Modeling streamflow driven by climate change in data-scarce mountainous basins. *Sci. Total Environ.* **2021**, *790*, 148256. [CrossRef]
85. Li, N.; McLaughlin, D.; Kinzelbach, W.; Li, W.; Dong, X. Using an ensemble smoother to evaluate parameter uncertainty of an integrated hydrological model of Yanqi basin. *J. Hydrol.* **2015**, *529*, 146–158. [CrossRef]